Innovation in metallurgical industrial and laboratory equipment, technologies and materials

Инновации в металлургическом промышленном и лабораторном оборудовании, технологиях и материалах

UDC 620.18
DOI 10.17073/0368-0797-2023-3-367-375

Original article
Оригинальная статья

A method for studying the frequency stability of materials during tests for multi-cycle fatigue of steel

V. V. Myl'nikov[1] ✉, **E. A. Dmitriev**[2]

[1] **Nizhny Novgorod State University of Architecture, Building and Civil Engineering** (65 Il'inskaya Str., Nizhny Novgorod 603950, Russian Federation)
[2] **Komsomolsk-on-Amur State University** (27 Lenina Ave., Komsomolsk-on-Amur, Khabarovsk Territory 681013, Russian Federation)

✉ mrmylnikov@mail.ru

Abstract. For trouble-free operation without loss of elastic and inelastic properties of particularly critical elements of electrical-to-mechanical vibration converters during a long period of cyclic operation, it is necessary, in addition to studying the fatigue characteristics of materials used for their manufacture, to study these alloys for frequency stability, since minor deviations in the frequency of natural oscillations lead to unacceptable errors in the operation of such high-precision products. To carry out such studies, we developed and constructed an original installation, in which sinusoidal loading is carried out according to the "soft" scheme of flat samples cantilever bending operating in self-oscillation mode. The frequency of cyclic loading in this installation is generated by current pulses, which are a response to the frequency of the test sample natural oscillations converted using electronics. As a result, frequency equality is achieved in the test process. An algorithm for calculating stresses depending on the loading amplitude of steel samples of different geometric shapes was developed. It is shown that the stress on the sample calculated by the deformation amplitude in all cases is 8 – 10 % higher than the stress calculated by the force, regardless of the shape of the proposed samples. To verify the proposed research method, martensitic-aging steel was tested at loads close to the fatigue limit, since frequency stability in this range is of great interest. We obtained the frequency characteristics in the multi-cycle test area. It was determined that with an operating time of 50 million loading cycles, the frequency change was 0.75 Hz. The dynamics of frequency stability was revealed: the frequency changed most intensively during the first 10 million loading cycles, during this time the frequency changed by 0.54 Hz.

Keywords: steel, fatigue, strain amplitude, loading frequency, durability, natural oscillation frequency, cyclic strength, frequency stability

For citation: Myl'nikov V.V., Dmitriev E.A. A method for studying the frequency stability of materials during tests for multi-cycle fatigue of steel. *Izvestiya. Ferrous Metallurgy*. 2023;66(3):367–375. https://doi.org/10.17073/0368-0797-2023-3-367-375

Метод изучения частотной стабильности материалов при испытаниях на многоцикловую усталость стали

В. В. Мыльников[1] ✉, **Э. А. Дмитриев**[2]

[1] **Нижегородский государственный архитектурно-строительный университет** (Россия, 603950, Нижний Новгород, ул. Ильинская, 65)
[2] **Комсомольский-на-Амуре государственный университет** (Россия, 681013, Хабаровский край, Комсомольск-на-Амуре, пр. Ленина, 27)

✉ mrmylnikov@mail.ru

Аннотация. Для безаварийного функционирования и без потерь упругих и неупругих свойств особо ответственных элементов преобразователей электрических колебаний в механические в течение длительного периода циклической наработки необходимо, кроме исследования усталостных характеристик материалов, применяемых для их изготовления, исследовать эти сплавы и на частотную стабильность. Это связано с тем, что незначительные отклонения частоты собственных колебаний приводят к недопустимым погрешностям в работе такого рода высокоточных изделий. Для проведения исследований разработана и сконструирована оригинальная установка, работающая в режиме автоколебаний, в которой осуществлено синусоидальное нагружение плоских образцов по «мягкой» схеме консольного изгиба. Частота циклического нагружения в установке генерируется импульсами тока, которые являются откликом на частоту собственных колебаний испытываемого образца, преобразованных с помощью электроники. В результате достигается частотное равенство в процессе

испытаний. Разработан алгоритм расчета напряжений в зависимости от амплитуды нагружения образцов из стали разной геометрической формы. Показано, что напряжение на образце, рассчитанное по амплитуде деформации, во всех случаях на 8 – 10 % выше напряжения, рассчитанного по силе вне зависимости от формы образцов. Для верификации предложенного метода исследований проведены испытания мартенситно-стареющей стали на нагрузках, близких к пределу усталости, так как наибольший интерес представляет стабильность частоты в этом диапазоне. Получены частотные характеристики в многоцикловой области испытаний. Определено, что при наработке в 50 млн циклов нагружения изменение частоты составило 0,75 Гц. Выявлена динамика частотной стабильности: наиболее интенсивно частота менялась при первых 10 млн циклов нагружения, за это время она изменилась на 0,54 Гц.

Ключевые слова: сталь, усталость, амплитуда деформации, частота нагружения, долговечность, частота собственных колебаний, циклическая прочность, стабильность частоты

Для цитирования: Мыльников В.В., Дмитриев Э.А. Метод изучения частотной стабильности материалов при испытаниях на многоцикловую усталость стали. *Известия вузов. Черная металлургия*. 2023;66(3):367–375. https://doi.org/10.17073/0368-0797-2023-3-367-375

Introduction

Standard fatigue tests serve the purpose of determining the mechanical properties of a material [1]. Engineers rely on these test results for material selection and structural analysis [2].

Several cyclic test procedures exist [3 – 6]. The essential fatigue test properties to accurately simulate the part's operating stress and strain [7 – 10] are as follows:

– loading program determined by the cycle amplitude form (Fig. 1);

– load scheme (Fig. 2);

– testing to a specified stress (σ, MPa) (Fig. 2, *a*) or strain (ε, mm) (Fig. 2, *d*).

Mission-critical components undergo validation using dedicated testing machines and specialized testing procedures. For example, materials with low inelastic pro-

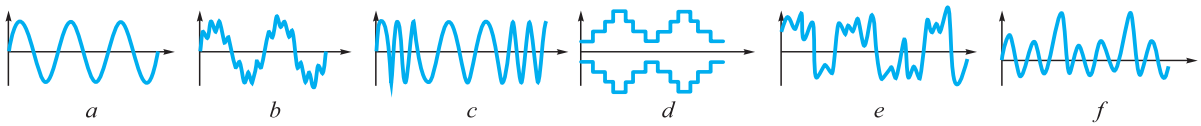

Fig. 1. Varieties of cycle amplitude forms:
a – sinusoidal cycle form (harmonic) with constant amplitude values; *b* – biharmonic; *c* – with variable frequency; *d* – programmed block cycle; *e* – with reproduction of the operational spectrum with time variable σ_a, with or without truncation of low σ_a; *f* – harmonic cycle with single overloads

Рис. 1. Разновидности форм амплитуд циклов:
a – синусоидальная форма цикла (гармоническая) с постоянными амплитудными значениями; *b* – бигармоническая; *c* – с переменной частотой; *d* – программированный блочный цикл; *e* – с воспроизведением эксплуатационного спектра с переменной во времени σ_a с усечением низких σ_a или без их усечения; *f* – гармонический цикл с одиночными перегрузками

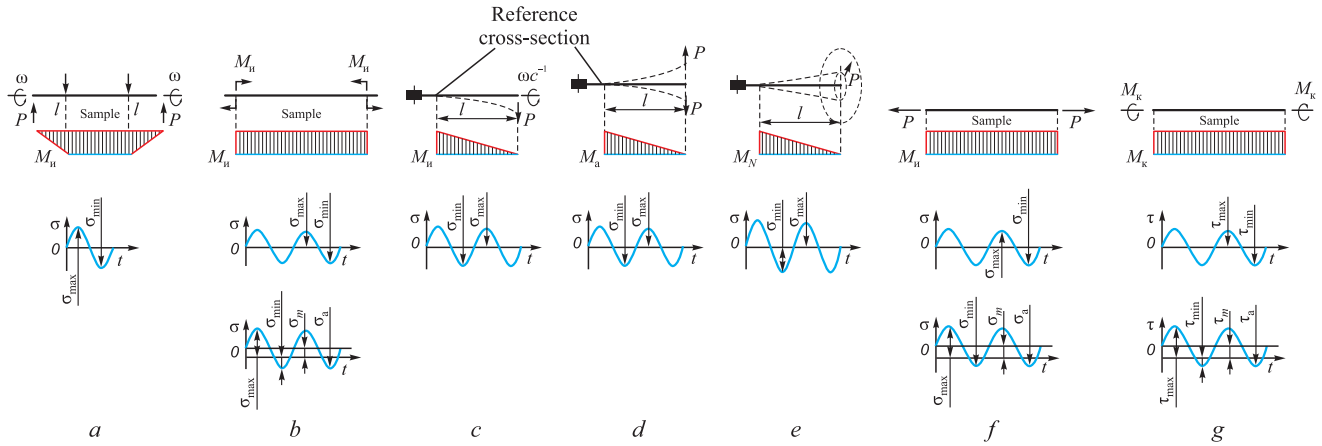

Fig. 2. Loading schemes during fatigue tests:
a – pure bending of a rotating cylindrical sample; *b* – pure bending in one plane; *c* – cantilever bending of a rotating cylindrical sample; *d* – cantilever cyclic transverse bending of a flat sample; *e* – transverse bending during rotation of the force plane; *f* – axial stretching along a pulsating cycle; *g* – alternating torsion

Рис. 2. Схемы нагружения при испытаниях на усталость:
a – чистый изгиб вращающегося цилиндрического образца; *b* – чистый изгиб в одной плоскости; *c* – консольный изгиб вращающегося цилиндрического образца; *d* – консольный циклический поперечный изгиб плоского образца; *e* – поперечный изгиб при вращении силовой плоскости; *f* – осевое растяжение по пульсирующему циклу; *g* – знакопеременное кручение

perties are required to make parts exposed to complex cyclic loading and dimensionally stable components. The inelastic properties exhibited during cyclic loading can be described as “internal friction”, “imperfect elasticity”, “damping", “mechanical hysteresis”, or “energy dissipation” [11]. It is commonly assumed in most studies that microplastic deformations under cyclic loading are localized and unevenly distributed due to the heterogeneity of the material‘s micro-properties. Another test involves measuring the mechanical properties at different temperatures to determine the elastic limit and activation energy of the micro deformations [12 – 15].

The objective of this study is to develop a testing procedure for estimating the frequency stability in elastic elements used in high-precision oscillators that convert electrical vibrations into mechanical oscillations. Even slight changes in frequency of natural oscillations (eigenfrequencies) caused by variations in the elastic modulus, material inelasticity, and of atomic and lattices vibrations can result in unacceptable errors in electric-to-mechanical oscillation conversion and premature fatigue failure [16 – 19].

Materials and Methods

A frequency stability testing installation was developed as shown in Fig. 3, designed specifically for conducting tests under unique stress conditions. This testing apparatus involved the application of isothermal cyclic loading to a flat cantilever sample, referred to as the “soft test” [20]. It employed an electromechanical oscillator with mechanical vibration frequency precisely aligned to the sample’s eigenfrequency, facilitating resonance oscillations.

The installation comprised three distinct components arranged separately:

– bed: this component supported both the sample and the electromagnetic exciter;

– power supply and automation unit: responsible for powering the electromagnetic exciter coil, this unit adjusted the amperage and frequency as needed;

– measurement system for monitoring oscillatory parameters.

The bed, a robust L-shaped metal structure, was installed on vibration isolators. It facilitated the transfer of sample oscillations to the piezoelectric accelerometer. The operation of the installation proceeded as follows: the sensor’s signal was transmitted to the power supply and automation unit, which then supplied the electromagnetic exciter coil with a frequency matching the sample’s eigenfrequency. To prevent the overlap of vibrational waves and enhance oscillation transfer, the bed and the coil (assembled with the stator at one end of the electromagnetic exciter armature) were isolated from each other using vibration isolators (antivibration pads).

The electromagnetic exciter coil is energized by current pulses supplied from the power supply (Fig. 3, *a*). These pulses induce an electromagnetic force that causes

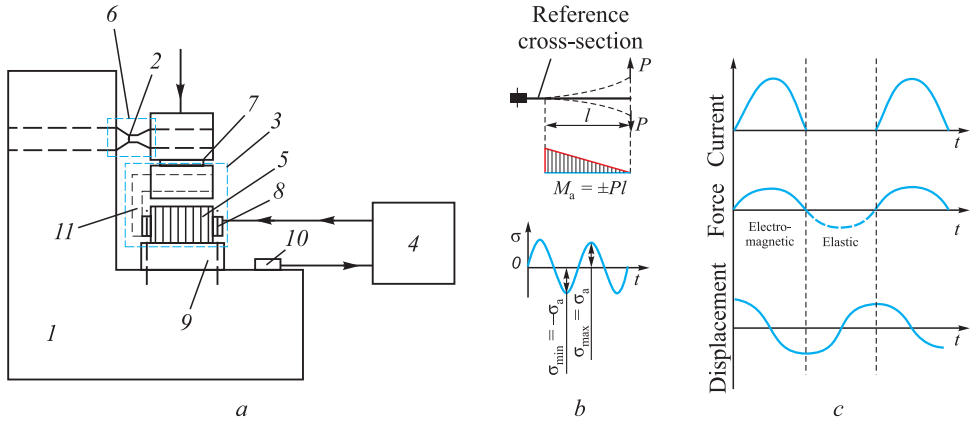

Fig. 3. Diagrams:
a – frequency stability testing installations: *1* – bed; *2* – sample; *3* – electromagnetic exciter; *4* – power supply and automation unit; *5* – coil of electromagnetic exciter; *6* – means of measuring parameters of the oscillatory process; *7* – ferromagnetic armature of electromagnetic exciter; *8* – electromagnetic stator exciter; *9* – vibration isolators; *10* – vibration acceleration sensor; *11* – *U*-shaped ribbon core; *b* – loads during cantilever cyclic transverse bending of a flat sample; *c* – matching current pulses, electromagnetic force and elastic force with movement of the console of the test sample in this installation

Рис. 3. Схемы:
a – установки для испытаний на частотную стабильность: *1* – станина; *2* – образец; *3* – электромагнитный возбудитель; *4* – блок питания и автоматики; *5* – катушка электромагнитного возбудителя; *6* – средство измерения параметров колебательного процесса; *7* – ферромагнитный якорь электромагнитного возбудителя; *8* – статор электромагнитного возбудителя; *9* – виброизоляторы; *10* – датчик виброускорения; *11* – П-образный ленточный сердечник; *b* – нагрузки при консольном циклическом поперечном изгибе плоского образца; *c* – согласования импульсов тока, электромагнитной силы и силы упругости с перемещением консоли исследуемого образца в данной установке

the armature, along with the sample, to move downward. the When the current is interrupted, the elastic force reinstates the sample to its original position, subjecting it to cyclic loading. The displacement curve of the sample's end is illustrated in Fig. 3, *c*. As fatigue advances, the eigenfrequency of the sample undergoes changes, consequently modifying the frequency of cyclic loading.

Through a series of comprehensive tests, we estimated the fatigue properties, frequency characteristics under cyclic loading, and determined the endurance limit. The frequency characteristics also serve as an indicator of the sample's rate of damage and enables estimation of its remaining lifespan [21].

The following variables were measured in our experiments:

– frequency;

– number of load cycles;

– amplitude of oscillations (measured through an optical sensor);

– amplitude of oscillations (measured via a photoelectric sensor);

– amplitude of oscillations (measured using a piezoelectric accelerometer);

– average current within the exciter coil circuit;

– the waveforms were visualized using an oscilloscope.

The samples illustrated in Fig. 4 were composed of the 03N18K9M5T-EL steel grade. The corresponding Table presents the dimensions of the samples.

We derived the stress within the sample's cross-section from the amplitude of oscillations. In order to gauge the stress, we established a correlation between the force applied to the sample and the displacement of the sample at the point of force application. Subsequently, the stress was calculated based on the force value. We also deduced the analytical relationship between force and displacement for the steady mode. It is assumed that during oscillations, the forces applied to the sample (external force, inertia, elastic force) generate the same maximum stress and maximum displacement (vibration amplitude) as the static force equivalent to the resultant dynamic force.

For the curved axis of a variable cross-section beam, we employed an approximate differential equation:

$$EJ(x)\frac{d^2y}{dx^2} = M(x), \qquad (1)$$

where $J(x)$ represents the second area moment; E stands for Young's modulus; $M(x)$ denotes the bending moment; y is the coordinate in the force direction; x is the coordinate along the beam axis.

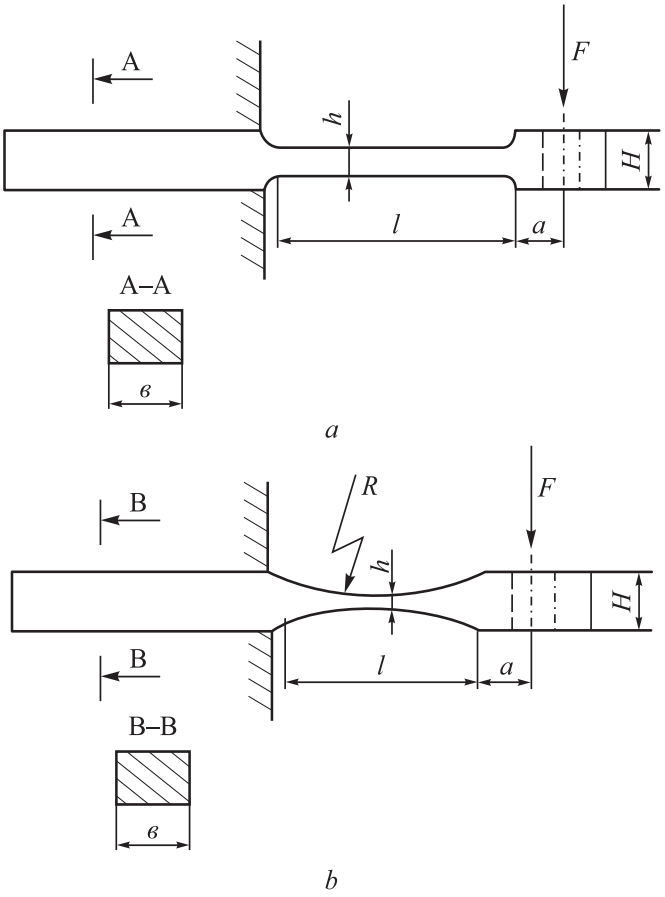

Fig. 4. Sketches of the samples:
a – flat samples; *b* – corset samples

Рис. 4. Эскизы образцов:
a – плоские образцы; *b* – корсетные образцы

Dimensions of fatigue test samples, mm

Размеры образцов для испытания на усталость, мм

Sample	*a*	*b*	*l*	*h*	*H*	*R*
a	10	22	43	5	13	–
*b*1	9	20	56	5	13	100
*b*2	24	20	56	5	13	100

Stress vs. Vibration Amplitude in Flat Samples

The eference point is located at the sample's restraint point. The bending moment at a distance x from the restraint point is givem by:

$$M = F(l + a - x). \qquad (2)$$

The displacement of the sample segment with a height h: $\frac{d^2y}{dx^2} = \frac{F(l+a-x)}{EJ_1}$, where $J_1 = \frac{bh^3}{12}$.

Initial conditions are: $x = 0$; $y_1 = 0$; $\frac{dy_1}{dx} = 0$.

A solution for the specified initial conditions is:

$$\begin{cases} \frac{dy_1}{dx} = \frac{F}{EJ_1} x\left(l + a - \frac{x}{2}\right); \\ y_1 = \frac{F}{EJ_1}\frac{x^2}{2}\left(l + a - \frac{x}{3}\right). \end{cases} \quad (3)$$

An equation for the displacement of the sample segment with height H: $\frac{d^2y_2}{dx^2} = \frac{F(l+a-x)}{EJ_2}$, where $J_2 = \frac{bH^3}{12}$.

The solution is:

$$\begin{cases} \frac{dy_2}{dx} = \frac{F}{EJ_2} x\left(l + a - \frac{x}{2}\right) + C_1; \\ Y_2 = \frac{F}{EJ_2}\frac{x^3}{2}\left(l + a - \frac{x}{3}\right) + C_1X + C_2. \end{cases} \quad (4)$$

Initial conditions are: $x = l$; $\frac{dy_1}{dx} = \frac{dy_2}{dx}$; $y_1 = y_2$.

By substituting the values of $x = l$ into (3) and (4), and solving the equations, we obtain:

$$C_1 = \frac{F}{E} l\left(\frac{l}{2} + a\right)\left(\frac{1}{J_1} - \frac{1}{J_2}\right); \; C_2 = \frac{F}{E}\frac{l^2}{2}\left(\frac{l}{3} + a\right)\left(\frac{1}{J_1} - \frac{1}{J_2}\right).$$

Using the constants the C_1 and C_2, along with the equation for y_2 derived from (4), we are able to determine the maximum displacement at the point of force application for $x = l + a$:

$$A_m = \frac{F}{EJ_2}\frac{(l+a)^3}{3} + \frac{F}{E} l(l+a)\left(\frac{l}{a} + a\right)\left(\frac{1}{J_1} - \frac{1}{J_2}\right) - \\ - \frac{F}{E}\frac{l^2}{2}\left(\frac{l}{3} + a\right)\left(\frac{1}{J_1} - \frac{1}{J_2}\right).$$

Given the provided values of h and H, where $J_2 \gg J_1$ ($J_1 = 208.3$ mm^4; $J_2 = 3662$ mm^4), taking into account this inequality and disregarding the inherent bending of the heightened sample segment with height H, we arrive at a more straightforward expression:

$$A_m = \frac{Fl}{EJ_1}\left(a^2 + la + \frac{l^2}{3}\right). \quad (5)$$

The stress at the reference cross-section (the restraint point) is: $\sigma = \frac{F(l+a)}{W}$.

By expressing F from (5) and taking into account that $\frac{J_1}{W} = \frac{h}{2}$, we obtain the final expression:

$$\sigma = \frac{1{,}5h(l+a)}{l\left(3a^2 + 3la + e^2\right)} EA_m. \quad (6)$$

For the sample dimensions indicated in Fig. 4, *a*, we get: $\sigma = 26.9 \cdot 10^{-5} EA_m$.

For the average Young's modulus $E = 2 \cdot 10^5$ MPa: $\sigma = 53.8A_m$, where σ is measured in MPa, A_m in mm.

Stress vs. Vibration Amplitude in Corset Samples

We approached the analysis of displacements separately for the curved and thickened segments.

To estimate the displacement of the curved segment, we positioned the origin in the midpoint of this segment (at $l/2$ from the restraint point). Consequently, the height of the cross-section at a distance x from the origin is given by:

$$h(x) = h + \left(R - \sqrt{R^2 - x^2}\right). \quad (7)$$

The bending moment at x is: $M(x) = F\left(\frac{l}{2} + a - x\right)$.

The equation for the displacement is derived from equation (1) by substituting $J_1 = \frac{bh^3(x)}{12}$. This is further supplemented by $h(x)$ from equation (7).

The resultant equation is:

$$\frac{d^2y_1}{dx^2} = \frac{1{,}5F}{bE} \frac{0{,}5l + a - x}{\left(0{,}5h + R - \sqrt{R^2 - x^2}\right)^3}. \quad (8)$$

The value of x is in the range: $-\frac{l}{2} \le x \le l_2$.

A computer-generated solution of differential equation (8) for $x = 0.5l$: produces the displacement y_{1m} and angle $\theta_{1m} = \frac{dy_1}{dx}$.

For the estimation of the displacement of the thickened segment, we positioned the origin at a distance l from the sample's restraint point.

The equation describing the displacement of this segment is: $\frac{d^2y_2}{dx^2} = \frac{F(a-x)}{EJ_2}$, where $J_2 = \frac{bH^3}{12}$.

The solution for this equation is:

$$\left.\begin{aligned} \frac{dy_2}{dx} &= \frac{F}{EJ_2} x\left(a - \frac{x}{2}\right) + C_1; \\ y_2 &= \frac{F}{EJ_2}\frac{x^2}{2}\left(a - \frac{x}{3}\right) + C_1x + C_2, \end{aligned}\right\} \quad (9)$$

where $0 \le x \le a$.

Initial conditions are: $x = 0$; $\theta_{1m} = \frac{dy_2}{dx}$; $y_2 = y_{1m}$.

Resulting in $C_1 = \theta_{1m}$; $C_2 = y_{1m}$.

By substituting $x = a$ into (9), we find y_2 at the point of force application, which is the amplitude of oscillations: $A_m = \frac{F}{EJ_2}\frac{a^3}{2} + \theta_{1m}a + y_{1m}$.

Due to the substantial value of J_2, the first term of this expression is significantly smaller compared to the other two and can be disregarded.

Let us denote θ'_{1m} and Y'_{1m} the values derived from equation (9) for $\frac{1,5F}{bE}=1$.

Then $\theta_{1m}=\theta'_{1m}\frac{1,5F}{bE}$; $y_{1m}=y'_{1m}\frac{1,5F}{bE}$.

The amplitude of oscillations is:

$$A_m=\frac{1,5F}{bE}\left(\theta'_{1m}a+y'_{1m}\right). \quad (10)$$

The stress in the sample cross-section at the center of the curved segment: $\sigma=\frac{F(0,5l+a)}{W}$.

By expressing F from equation (10) and considering $W=\frac{bh^2}{6}$, we arrive the final expression:

$$\sigma=\frac{2(l+2a)}{h^2\left(\theta'_{1m}a+y'_{1m}\right)}EA_m. \quad (11)$$

The problem was addressed through numerical solutions. Computer calculations for the *b*1 and *b*2 samples (with dimensions provided in the table and Fig. 4) yielded:

– sample *b*1: $\theta'_{1m}=59.84$; $y'_{1m}=1853.2$;

– sample *b*2: $\theta'_{1m}=84.1$; $y'_{1m}=2532.4$.

From equation (11), we obtain:

– sample (*b*1): $\sigma=24.75\cdot10^{-3}EA_m$, MPa;

– sample (*b*2): $\sigma=18.3\cdot10^{-3}EA_m$, MPa.

Considering the average Young's modulus $E=2\cdot10^5$ MPa:

– $\sigma=49.5A_m$ for sample *b*1;

– $\sigma=36.6A_m$ for sample *b*2.

Here, σ is measured in MPa and A_m in mm.

Error Estimation of the Stress Value in the Reference Cross-Section

If direct measurement errors for variations in Young's modulus and the geometric dimensions of the sample are available, we can estimate the error of the indirectly measured σ as stated in equation (6)

$$\frac{\Delta\sigma}{\sigma}=\delta_A+\delta_E+\delta_e, \quad (12)$$

where $\delta_E=\frac{\Delta E}{E}$ is the relative error of Young's modulus;

$\delta_A=\frac{\Delta A}{A}$ is the relative error of the amplitude;

$$\delta_e=\frac{\Delta h}{h}+\left[\frac{1}{a+l}+\frac{1}{l}+\frac{2l+3a}{3\left(a^2+ab+\frac{l^2}{3}\right)}\right]\Delta l+$$
$$+\left(\frac{1}{a+l}+\frac{l+2a}{a^2+al+\frac{l^2}{3}}\right)\Delta a- \quad (13)$$

is the relative error of the sample's dimensions.

The relative error of the amplitude of oscillations has been previously determined as: $\delta_A=0.01$ (1 %).

The relative error of the sample's linear dimensions is estimated as (13):

$$\delta_e=0.0123\ (1.23\ \%). \quad (14)$$

There is inherent uncertainty in the value of Young's modulus. Available sources specify that for high elastic steels, this value varies from $1.9\cdot10^5$ to $2.1\cdot10^5$ MPa. In this context $\Delta E=\pm10^4$ MPa should be considered as the error in Young's modulus:

$$\delta_E=0.05\ (5\ \%). \quad (15)$$

The total error of the estimated stress in the reference section is given by:

$$\frac{\Delta\sigma}{\sigma}=0.0723\ (7.23\ \%). \quad (16)$$

For validation purposes, we employed static calibration to estimate the stress in the sample. This involved applying static loading to the sample with the force F, measured using a reference dynamometer. The stress in the sample is then estimated from the force value using equation

$$\sigma=\frac{6F(l+a)}{bh^2}. \quad (17)$$

We simultaneously recorded readings from the reference dynamometer and the linear displacement gauge (which measured strain under load).

The following values were obtained:

$$\left.\begin{aligned}\sigma_A&=501A_m\cdot10^{-6},\ \text{Pa},\\ \sigma_F&=\frac{6(l+a)}{bh^2}F=0.596\cdot10^{-6}F,\ \text{Pa};\end{aligned}\right\}\ \text{for sample } a$$

$$\left.\begin{aligned}\sigma_A&=485A_m\cdot10^{-6},\ \text{Pa},\\ \sigma_F&=\frac{6(l/2+a)}{bh^2}F=0.444\cdot10^{-6}F,\ \text{Pa}.\end{aligned}\right\}\ \text{for sample } b$$

This reveals that stress values estimated from strain and measured by the reference dynamometer differ by no more than 10 %.

To assess this outcome, let us calculate the error of the stress value derived from equation (17). It is the sum of the force measurement error $\sigma_F = \frac{\Delta F}{F}$ and the sample's linear dimension error $\sigma_E = \frac{\Delta l + \Delta a}{l + a} + \frac{\Delta b}{b} \frac{z\Delta h}{h}$:

$$\frac{\Delta\sigma}{\sigma} = \delta_F + \delta_e. \quad (18)$$

Given that we measured the sample with a precise micrometer, $\Delta a = \Delta l = \Delta b = \Delta h = 0.01$ mm and $\delta_e = 0.00075$ (0.075 %), which is a very low error. The primary contributor to the total error is the force measurement by the reference dynamometer, which is approximately 1 % and corresponds to the instrument's calibration error.

The stress calculated from strain σ_A is 8 – 10 % higher than the stress calculated from the force σ_F for both samples depicted in Fig. 4, *a* and *b*. This divergence can be attributed to several factors: the error in Young's modulus value; the assumptions made when deriving the equations for σ_A and systematic error overlooked during instrument calibration.

Results and Discussion

We employed the proposed procedure to conduct a test a sample composed of 03H18K9M5T-EL steel grade (Fig. 4, *a*). The focal point of our investigation lies in the frequency stability when subjected to loads near the fatigue limit. We scrutinized the frequency characteristics of a sample under 670 MPa load applied at ~200 Hz. Notably, the frequency deviation from the initial value displayed an upward trend denoted by positive values and a downward trend with negative values. The sample underwent a total of 50 million loading cycles. The maximum frequency deviation recorded was 0.75 Hz, making it the most stable frequency among all the samples. Interestingly, a significant frequency shift was observed within the initial 10 million load cycles, amounting to 0.54 Hz. The sample underwent continuous testing, with a load cycle of 10 million cycles per day. The frequency of the sample exhibited changes following overnight interruptions. Specifically, after a 10-hour pause, the morning frequency surpassed the frequency recorded the night before.

In Fig. 5, *a*, two envelope curves are depicted. Curve *1* portrays the frequency when the testing installation is operational, while Curve *2* represents the frequency once the testing installation is halted after daily operation. Curve *1* delineates the alteration in the initial frequency ("on" frequency), whereas Curve *2* showcases the modification in the final frequency ("off" frequency). The daily fluctuations in frequency during the cyclic testing period fall within the range delineated by the two curves.

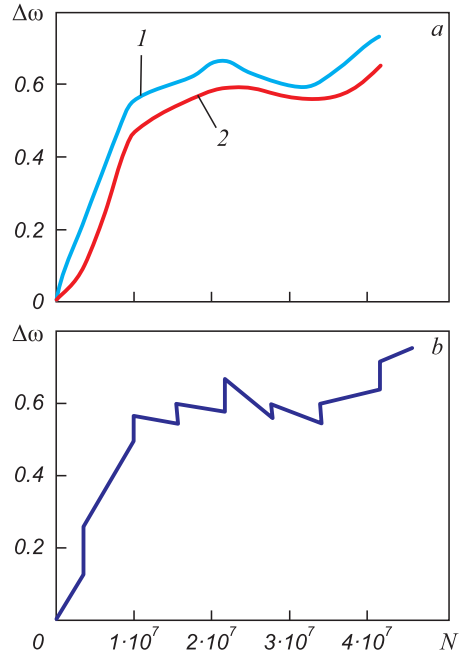

Fig. 5. Frequency characteristics during cyclic loading with interruptions in tests:
1 – frequency at the moment of switching on;
2 – frequency at the moment of shutdown

Рис. 5. Частотные характеристики при циклическом нагружении с перерывами в испытаниях:
1 – частота в момент включения; *2* – частота в момент отключения

Another frequency response is illustrated in Fig. 5, *b*, represented by a discontinuous line. The vertical steps correspond to frequency shifts following overnight interruptions. The sloped lines indicate daily frequency variations as the number of load cycles increases.

Conclusions

We proposed a procedure along with equations to estimate stresses on steel samples of various shapes. This estimation allows us to assess the frequency characteristic alterations during cyclic loading, following the "soft" cantilever bending scheme applied to flat samples with sinusoidal loading. This approach proves to be an effective tool for analyzing the frequency stability and variations in non-continuous fatigue tests. Moreover, it can be employed to gauge material internal friction and energy dissipation, facilitating the determination of damping capacity.

References / Список литературы

1. Shkol'nik L.M. *Fatigue Testing Methodology. Guide*. Moscow: Metallurgiya; 1978:304. (In Russ.).
Школьник Л.М. *Методика усталостных испытаний: Справочник*. Москва: Металлургия; 1978:304.
2. Gadolina I.V., Makhutov N.A., Erpalov A.V. Varied approaches to loading assessment in fatigue studies. *International Journal of Fatigue*. 2021;144:106035. https://doi.org/10.1016/j.ijfatigue.2020.106035

3. Suresh S. *Fatigue of Metals*. Cambridge University Press; 2006:701.

4. Terent'ev V.F., Korableva S.A. *Fatigue of Metals*. Moscow: Nauka; 2015:479. (In Russ.).

Терентьев В.Ф., Кораблева С.А. *Усталость металлов*. Москва: Наука; 2015:479.

5. Gromov V.E., Ivanov Yu.F., Vorobiev S.V., Konovalov S.V. *Fatigue of Steels Modified by High Intensity Electron Beams*. Cambridge; 2015:272.

6. Mughrabi H., Christ H.-J. Cyclic deformation and fatigue of selected ferritic and austenitic steels; specific aspects. *ISIJ International*. 1997;37(12):1154–1169. https://doi.org/10.2355/isijinternational.37.1154

7. Gadenin M.M. Study on damaging and fatigue life of constructions under single- and two-frequency loading modes based on deformational and energy approaches. *Inorganic Materials*. 2018;54(15):1543–1550. https://doi.org/10.1134/S0020168518150049

8. Gadenin M.M. Influence of loading cycle form on resistance to cyclic deformation and destruction of structural materials. *Vestnik nauchno-tekhnicheskogo razvitiya*. 2010;(9(37)): 15–19. (In Russ.).

Гаденин М.М. Влияние формы цикла нагружения на сопротивление циклическому деформированию и разрушению конструкционных материалов. *Вестник научно-технического развития*. 2010;(9(37)):15–19.

9. Myl'nikov V.V., Shetulov D.I., Kondrashkin O.B., Chernyshov E.A., Pronin A.I. Changes in fatigue resistance of structural steels at different loading spectra. *Izvestiya. Ferrous Metallurgy*. 2019;62(10):796-802. (In Russ.). https://doi.org/10.17073/0368-0797-2019-10-796-802

Мыльников В.В., Шетулов Д.И., Кондрашкин О.Б., Чернышов Е.А., Пронин А.И. Изменение показателей сопротивления усталости конструкционных сталей при различных спектрах нагружения. *Известия вузов. Черная Металлургия*. 2019;62(10):796–802. https://doi.org/10.17073/0368-0797-2019-10-796-802

10. Gadenin M.M. Calculation-and-experimental estimation of the role of the frequency ratio in changing the endurance at two-frequency deformation modes. *Zavodskaya laboratoriya. Diagnostika materialov*. 2019;85(1-1):64–71. (In Russ.). https://doi.org/10.26896/1028-6861-2019-85-1-I-64-71

Гаденин М.М. Расчетно-экспериментальная оценка роли соотношения частот в измерении долговечности при двухчастотных режимах деформирования. *Заводская лаборатория. Диагностика материалов*. 2019; 85(1–1):64–71. https://doi.org/10.26896/1028-6861-2019-85-1-I-64-71

11. Troshchenko V.T., Khamaza L.A., Pokrovsky V.V., etc. *Cyclic Deformation and Fatigue of Metals*. Bily M. ed. Amsterdam: Elsevier; 1993:500.

12. Golovin S.A., Tikhonova I.V. Temperature dependence of internal friction and properties of deformed low-carbon iron alloys. *Deformatsiya i razrushenie materialov*. 2013;(7): 16–21. (In Russ.).

Головин С.А., Тихонова И.В. Температурная зависимость внутреннего трения и свойства деформированных малоуглеродистых сплавов железа. *Деформация и разрушение материалов*. 2013;(7):16–21.

13. Golovin S.A., Petrushina A.G. Temperature spectrum of internal friction of cast iron. *Izvestiya. Ferrous Metallurgy*. 2009;52(9):51–54. (In Russ.).

Головин С.А., Петрушина А.Г. Температурный спектр внутреннего трения чугунов. *Известия вузов. Черная металлургия*. 2009;52(9):51–54.

14. McClaflin D., Fatemi A. Torsional deformation and fatigue of hardened steel including mean stress and stress gradient effects. *International Journal of Fatigue*. 2004;26(7):773–784. https://doi.org/10.1016/j.ijfatigue.2003.10.019

15. Golovin I.S., Bychkov A.S., Mikhailovskaya A.V., Dobatkin S.V. Contributions of phase and structural transformations in multicomponent Al-Mg alloys to the linear and nonlinear mechanisms of anelasticity. *The Physics of Metals and Metallography*. 2014;115(2):192–201. https://doi.org/10.1134/S0031918X14020082

Головин И.С., Бычков А.С., Михайловская А.В., Добаткин С.В. Вклад фазовых и структурных превращений в многокомпонентных AL-MG сплавах в линейные и нелинейные механизмы неупругости. *Физика металлов и металловедение*. 2014;115(2):204. https://doi.org/10.7868/ S0015323014020089

16. Kardashev B.K., Sapozhnikov K.V., Betekhtin V.I., Kadomtsev A.G., Narykova M.V. Internal friction, Young's modulus, and electrical resistivity of submicrocrystalline titanium. *Physics of the Solid State*. 2017;59(12):2381–2386. https://doi.org/10.1134/S1063783417120204

17. Blanter M.S., Golovin I.S., Neuhäuser H., Sinning H.R. Internal friction in metallic materials. *Springer Series in Materials Science*. 2007;90:1–535. https://doi.org/10.1007/978-3-540-68758-0

18. Stolyarov V.V. Inelasticity of ultrafine-grained metals. *Izvestiya. Ferrous Metallurgy*. 2010;53(11):51–54. (In Russ.).

Столяров В.В. Неупругость ультрамелкозернистых металлов. *Известия вузов. Черная металлургия*. 2010;53(11): 51–54.

19. Romaniv O.N., Laz'ko L.P., Krys'kiv A.S. Relationship of internal friction to the fatigue life of patented steel wire. *Soviet Mater Science*. 1984;19:522–527. https://doi.org/10.1007/BF00722120

20. Myl'nikov V.V., Shetulov D.I. *Installation for fatigue testing*. Patent RF no. 2781466. *Bulleten' izobretenii*. 2022;(29). (In Russ.).

Пат. 2781466 RU. *Установка для испытаний на усталость* / Мыльников В.В., Шетулов Д.И.; заявл. 14.09.2021; опубл. 12.10.2022. Бюл. № 29.

21. Demidov A.S., Kashelkin V.V. Determination of damage and stress state of beam samples by changing the natural frequency and amplitude of vibrations. *Vestnik Moskovskogo aviatsionnogo instituta*. 2009;16(3):62–64. (In Russ.).

Демидов А.С., Кашелкин В.В. Определение поврежденности и напряженного состояния балочных образцов по изменению собственной частоты и амплитуды колебаний. *Вестник Московского авиационного института*. 2009;16(3):62–64.

Information about the Authors / Сведения об авторах

Vladimir V. Myl'nikov, *Cand. Sci. (Eng.), Assist. Prof. of the Chair "Building Technology",* Nizhny Novgorod State University of Architecture, Building and Civil Engineering
ORCID: 0000-0001-5545-4163
E-mail: mrmylnikov@mail.ru

Eduard A. Dmitriev, *Dr. Sci. (Eng.), Assist. Prof., Rector,* Komsomolsk-on-Amur State University
ORCID: 0000-0001-8023-316X
E-mail: rector@knastu.ru

Владимир Викторович Мыльников, *к.т.н., доцент кафедры «Технологии строительства»,* Нижегородский государственный архитектурно-строительный университет
ORCID: 0000-0001-5545-4163
E-mail: mrmylnikov@mail.ru

Эдуард Анатольевич Дмитриев, *д.т.н., доцент, ректор,* Комсомольский-на-Амуре государственный университет
ORCID: 0000-0001-8023-316X
E-mail: rector@knastu.ru

Received 12.02.2023
Revised 12.03.2023
Accepted 11.04.2023

Поступила в редакцию 12.02.2023
После доработки 12.03.2023
Принята к публикации 11.04.2023